Journal of Photochemistry, 5 (1976) 355 - 373

PHOTOLYSIS OF SULFUR DIOXIDE IN THE PRESENCE OF FOREIGN GASES: VII. ACETYLENE

NELSON KELLY, JAMES F. MEAGHER and JULIEN HEICKLEN
Department of Chemistry and Center for Air Environment Studies, The Pennsylvania State University, University Park, Pa. 16802 (U.S.A.)
(Received February 9, 1976)

Summary

SO_2 was photolyzed at 25 °C and 3130 Å in the presence of acetylene. The quantum yield of the sole gas-phase product, CO, was determined for a wide range of SO_2 and C_2H_2 pressures, and in the presence of CO_2, NO and H_2O. The quantum yield, $\Phi\{CO\}$, increases with the ratio $[C_2H_2]/[SO_2]$ to an upper limiting value of 0.052. In the presence of excess CO_2 or H_2O vapor, $\Phi\{CO\}$ becomes independent of $[SO_2]$ and is reduced at low values of $[C_2H_2]$ but remains unchanged or increases slightly at high values of $[C_2H_2]$. As NO is added at the higher C_2H_2 pressures it first increases $\Phi\{CO\}$ but then reduces it to zero. None of the CO comes from singlet states as shown by the strong quenching of CO production by NO. Both of the two non-emitting triplet states previously proposed to be important in the photochemistry of SO_2, as well as the emitting triplet, are necessary to interpret the results of this study. A relatively complete mechanism is presented, all the pertinent rate coefficient ratios are obtained, and from these, values of $\Phi\{CO\}$ are computed. They agree well with the observed values.

Introduction

Although the primary photophysical processes of SO_2 have been studied for over a decade, they are still not clearly established. This is surprising since structurally SO_2 is a simple molecule. The demonstrated participation of both singlet and triplet states in the photochemistry as well as the fact that SO_2 absorbs up to 3900 Å make its study theoretically interesting as well as useful in understanding its role in atmospheric chemistry. Since radiation above 2200 Å possesses insufficient energy to rupture the S–O bond, photochemically induced reactions at $\lambda > 2200$ Å are the result of interactions with bound excited states.

Two emitting states of SO_2, a singlet designated $SO_2(^1B_1)$ and a triplet designated $SO_2(^3B_1)$ have been observed upon excitation into the region from 2500 to 3400 Å. The simplest interpretation is that the initial absorption is the $SO_2(^1B_1) \leftarrow SO_2(X, ^1A_1)$ transition, and $SO_2(^3B_1)$ is produced by intersystem crossing.

Many workers have studied the primary photophysical processes when SO_2 is excited into the singlet band centered at 2900 Å. Using emission lifetime measurements as well as fluorescence and phosphorescence quantum yields during steady state exposure, the details of the mechanism were proposed [1 - 10].

Excited SO_2 was shown to be chemically reactive and the reactions of SO_2 excited within the first allowed band with hydrocarbons and CO were studied by Dainton and Ivin [11,12], Timmons [13] and Calvert and coworkers [14]. The photosensitized *cis–trans* isomerization of butene-2 was studied by Cox [15], Penzhorn and Gusten [16], and Calvert and coworkers [17]. The reactivity of $SO_2(^3B_1)$ was demonstrated in the CO [18], paraffin [19], olefin [20] and aromatic hydrocarbon [21] systems by direct excitation into the triplet band in the Calvert laboratory.

The Calvert group also studied the phosphorescence decay of $SO_2(^3B_1)$ generated by intersystem crossing from the singlet [22] and direct excitation into the triplet band [23]. The quenching reactions of $SO_2(^1B_1)$ as well as the quenching of $SO_2(^3B_1)$ were also extensively studied using a variety of quenching molecules and conditions.

In this laboratory the photochemical interaction of SO_2 with CO [28, 29], C_2F_4 [28], thiophene [30] and biacetyl [31] have been investigated. The results are not consistent with a mechanism including only the emitting states. The participation of other states was invoked in order to explain the results. The postulated photochemical mechanisms require a non-emitting singlet designated SO_2^* as well as two non-emitting triplets designated SO_2^{**} and $SO_2^{\dagger}$. The mechanisms proposed accommodates the data obtained by other workers.

Since the fluorescence quantum yield was observed not to obey Stern–Volmer quenching, it seems that $SO_2(^1B_1)$ is not the state initially produced upon absorption. Moreover, since the phosphorescence quantum yield does obey Stern–Volmer quenching its sole precursor cannot be $SO_2(^1B_1)$ [32].

Brus and McDonald [33] found two fluorescing states when SO_2 was excited at 2600 - 3250 Å. The minor fluorescence was attributed to the $^1A_2$ state which has a lifetime of $\sim$50 μs and a bimolecular quenching rate that is an order of magnitude greater than the gas kinetic rate. The major fluorescence was interpreted in terms of extensive Renner rovibronic pertubation between an excited quasilinear $^1B_1$ state and the ground $^1A_1$ state.

There is theoretical evidence that many states of SO_2 are present in the wavelength region of interest [34] but only recently have these been invoked to explain the photochemistry. Recent attempts to explain energy

exchange in excited SO_2 have included the six low lying excited states $^{1,3}B_1$, $^{1,3}B_2$, $^{1,3}A_2$ [33, 35]. The Calvert group has also found it necessary to invoke an additional excited state of SO_2 to accommodate their data for various systems at high pressures [14, 17, 26, 36]. However, they have favored the possibility that this state is chemically inert and only serves as an additional source of $SO_2(^3B_1)$.

The present study involves the photolysis of SO_2 at 3130 Å in the presence of acetylene and various quenching gases. Previous studies by Luria *et al.* [37, 38] show CO and a solid aerosol to be the only products. It is believed that the quantum yield of CO will serve as a measure of the participation of the various possible reactive states and that the addition of quenching gases will permit the characterization of these states.

Experimental

All gases were supplied by Matheson Gas Products. Sulfur dioxide (anhydrous) was distilled once from −95° to −130 °C. The middle fraction was collected and placed in a darkened storage bulb. Acetylene and carbon dioxide (bone dry) were distilled from −130° to −196 °C. In each case the middle fraction was retained. Nitric oxide was passed through silica gel and distilled from −186° to −196 °C. The middle fraction was transferred to a darkened storage bulb. Gas chromatographic analysis showed only a small nitrogen impurity. Water (triple distilled and de-ionized) was degassed repeatedly at −196 °C. The azomethane was prepared from a procedure given by Renaud and Leitch [39]. It was purified by trap-to-trap distillation from −90° to −130 °C. All of the above gases were degassed at −196 °C immediately before use.

All experiments were carried out on a high vacuum line using Teflon stopcocks with Viton "O" rings. Pressures from 3 to 750 Torr were measured on 0 - 50 or 0 - 800 Torr Wallace and Tiernan absolute pressure gauges. A silicone oil manometer was employed for most pressure measurements below 10 Torr. In the case of water all measurements were made with this manometer. Pressures less than 0.5 Torr were achieved by expansion.

Photolysis was carried out in a cylindrical cell 50 cm × 5 cm o.d. with quartz windows bonded to both ends. A 6 mm o.d. perforated gas inlet tube passing down the length of the cell ensured thorough mixing when the gases were introduced. The radiation source was a Hanovia 140 W U-shaped mercury arc. The light was collimated by a quartz lens and passed through a Corning 7-54 (9863) glass filter and an Ealing 3130 Å interference filter before entering the cell. A phototube was placed at the opposite end of the cell to measure light intensity.

The reaction cell was connected to a Toepler pump through two spiral traps maintained at liquid nitrogen temperature. This allowed

non-condensable gas to be transferred to a gas buret where the pressure was measured. When all the gas was transferred, as evidenced by a constant-pressure reading, the gas was pushed into a gas chromatograph sample loop. A trap in solid nitrogen was used in place of the second spiral trap when NO was present.

A Gow Mac Model No. 40-012 gas chromatograph using a thermistor detector maintained at 0 °C was used for N_2, CO and NO analysis. A 5 ft, 1/4 in. o.d. copper column packed with 13X molecular sieves, maintained at room temperature and with a flow rate of 72 cm^3/min of helium, provided separation of non-condensable gases. The system was calibrated with standard samples of CO and blanks were performed with all the gases used.

Azomethane was used as the actinometer in this study. The quantum yield for N_2 formation is unity at 3130 Å. The nitrogen produced in azomethane photolysis was determined in the same manner as for CO using the gas buret and gas chromatograph. The gas chromatograph was calibrated for N_2 using standard samples. The phototube was used to match absorbances of SO_2 and $(CH_3)_2N_2$. This was checked for each run and each actinometer experiment. The amount of CO produced in each experiment was obtained and converted to a quantum yield using the nitrogen obtained from an azomethane experiment at matched absorbance.

Results

All experiments were carried out at 25 °C and 3130 Å. A SO_2 pressure of 2.7 Torr reduced the intensity of light reaching the phototube by about 50%. Carbon monoxide analyses were performed in identical experiments with various exposure times. Such experiments were done for a variety of reactant mixtures. In each of these sets the CO growth was linear and showed no detectable induction period or fall-off at longer exposures. This indicates that CO is an initial product and that there is not a significant amount of light scattering from the aerosol under the conditions we have employed.

A series of experiments were done at a SO_2 pressure of 2.6 ± 0.2 Torr and an acetylene pressure of 0.93 ± 0.01 Torr where the incident intensity was varied from 1.2 to 12.3 mTorr/min. There was no systematic variation in the results, and they were the same within the experimental scatter. For all the runs described below, with the exception of a few at high SO_2 pressures, I_a was between the above limits.

With the SO_2 pressure at 2.7 ± 0.2 Torr, the C_2H_2 pressure was varied from 1.58 mTorr to 718 Torr (Fig. 1, curve a). $\Phi\{CO\}$ increases proportionately with the C_2H_2 pressure at low C_2H_2 pressures, but the increase is much slower at higher C_2H_2 pressures. These results agree well with the more limited data of Luria and Heicklen [38]. Their $\Phi\{CO\}$ values were slightly higher but the shape of the curves checked well over

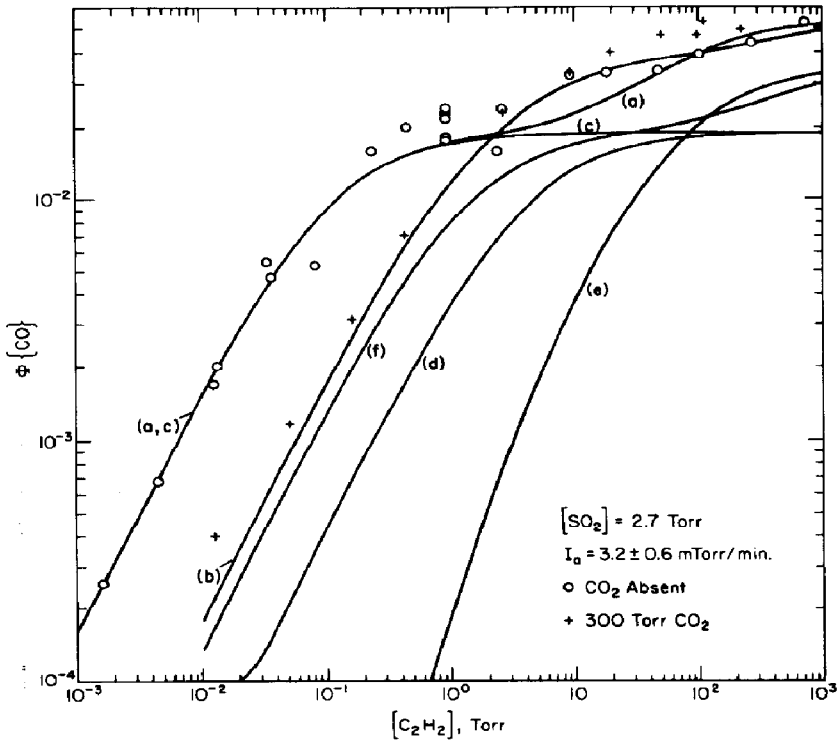

Fig. 1. Log–log plots of $\Phi\{CO\}$ *vs.* C_2H_2 pressure with and without 300 Torr of CO_2. The curves are theoretically computed from the rate coefficients listed in Table 1. (a) Total $\Phi\{CO\}$, no CO_2; (b) total $\Phi\{CO\}$, $[CO_2]$ = 300 Torr; (c) $\Phi^3\{CO\}$, no CO_2; (d) $\Phi^3\{CO\}$, $[CO_2]$ = 300 Torr; (e) $\Phi^{**}\{CO\}$, no CO_2; (f) $\Phi^{**}\{CO\}$, $[CO_2]$ = 300 Torr.

the range for which the data overlapped in the two studies. When the SO_2 pressure was varied from 0.09 to 20.0 Torr at a constant pressure of C_2H_2 of 0.93 ± 0.01 Torr, it was found that $\Phi\{CO\}$ is dependent on the $[SO_2]/[C_2H_2]$ ratio. The same ratio was produced with different combinations of reactant pressures and gave the same value for $\Phi\{CO\}$. Figure 2 shows that $\Phi\{CO\}^{-1}$ varies linearly with $[SO_2]/[C_2H_2]$.

Luria and Heicklen [38] previously reported no effect on $\Phi\{CO\}$ when an atmosphere of CO_2 was added to a mixture of 2.2 Torr of SO_2 and 2.2 Torr of C_2H_2. We duplicated this experiment and confirmed the results. However, when CO_2 is added to reactant mixtures containing 0.93 ± 0.01 Torr of C_2H_2 and 2.58 ± 0.15 Torr of SO_2, $\Phi\{CO\}$ decreases from 0.020 to 0.0123 with the addition of 96.4 Torr of CO_2, after which it is independent of CO_2 pressure (Fig. 3, middle curve). An even more dramatic reduction is observed at a C_2H_2 pressure of 0.086 ± 0.005 Torr and a SO_2 pressure of 2.71 ± 0.05 Torr (Fig. 3, lower curve). When CO_2 is added to a mixture containing 101 ± 3 Torr of C_2H_2 and 2.69 ± 0.10 Torr of SO_2, $\Phi\{CO\}$ is slightly enhanced (Fig. 3, upper curve).

Experiments were done with 2.62 ± 0.14 Torr of SO_2, 300 ± 3 Torr of CO_2 and varying C_2H_2 from 0.0130 Torr to 227 Torr (Fig. 1, curve b).

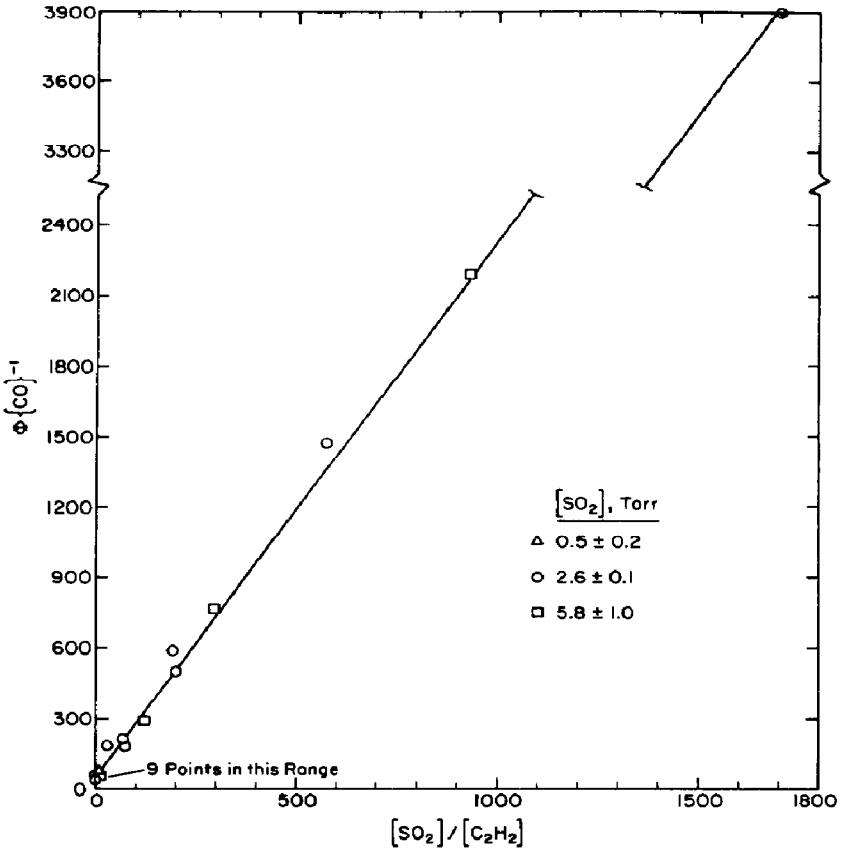

Fig. 2. Plot of reciprocal CO quantum yield *vs.* $[SO_2]/[C_2H_2]$ in the photolysis of SO_2–C_2H_2 mixtures at low total pressures.

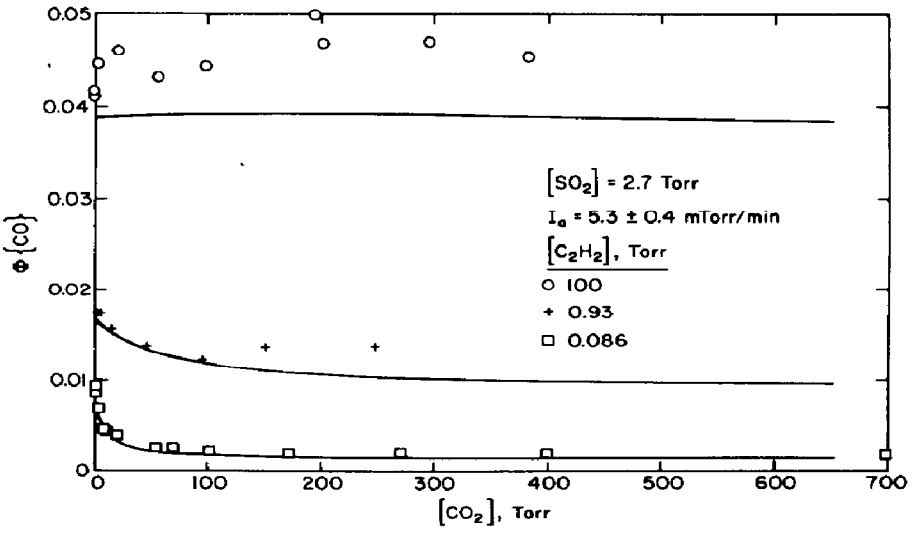

Fig. 3. Plots of $\Phi\{CO\}$ *vs.* the CO_2 pressure in the irradiation of SO_2–C_2H_2 mixtures in the presence of CO_2. The curves are theoretically computed from the rate coefficients listed in Table 1.

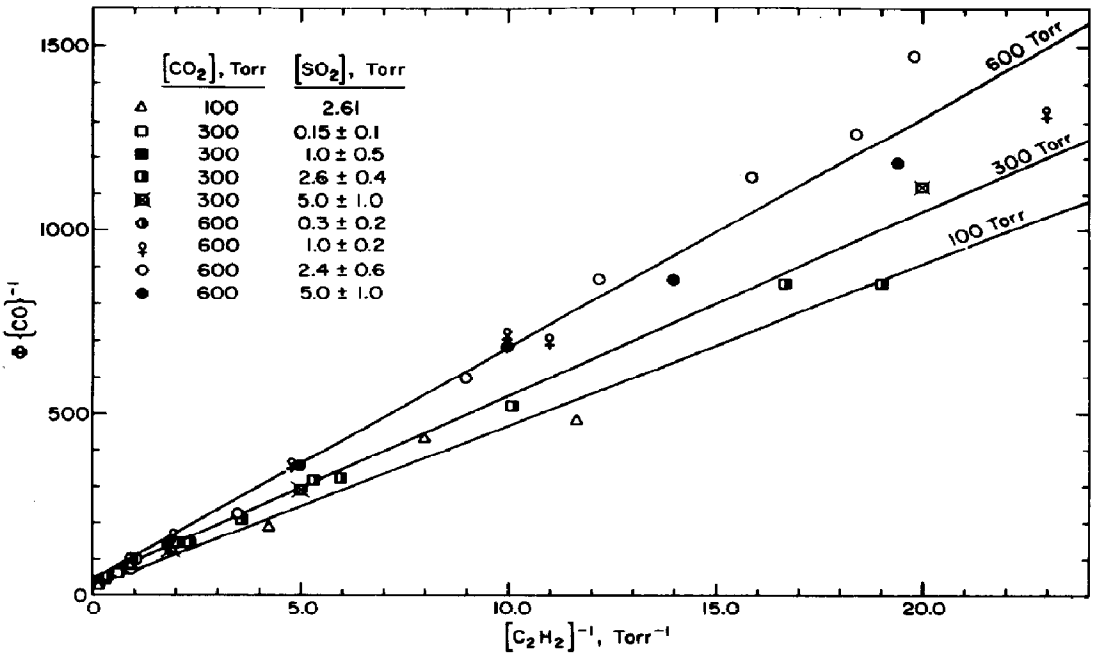

Fig. 4. Plots of reciprocal CO quantum yield *vs.* reciprocal C_2H_2 pressure at various CO_2 pressures.

From these data one can see that in previous work [38] the choice of experimental conditions was fortuitous in that for only a small range of reactant pressures around the one used is no CO_2 effect observed. The crossing point of the two curves corresponds almost exactly to experimental conditions of the earlier study. As can be seen from Fig. 3 the CO_2 effect is usually quite strong and can either reduce or increase the observed quantum yield.

When CO_2 was present at 300 or 600 Torr, $\Phi\{CO\}$ was found to be independent of $[SO_2]$ (Fig. 4). An extended series of runs varying $[C_2H_2]$ from 0.015 to 6 Torr with SO_2 from 0.1 to 6 Torr in the presence of 600 ± 10 Torr of CO_2 was completed (upper curve, Fig. 4). In the presence of 300 ± 5 Torr of CO_2 fewer runs were done with SO_2 varying from 0.1 to 6 Torr (middle curve, Fig. 4). A few runs were also done with only 100 Torr of CO_2 present at constant $[SO_2]$ (lower curve, Fig. 4). At each CO_2 pressure $\Phi\{CO\}^{-1}$ varies linearly with $[C_2H_2]^{-1}$.

Another series of runs with the SO_2 pressure at 2.7 Torr and with C_2H_2 at 0.086, 2.34 and 100 Torr were done with NO as the quenching gas. For the runs with 0.086 ± 0.002 Torr of C_2H_2, NO was added from 2.45 mTorr to 1 Torr and quenched $\Phi\{CO\}$ from 0.00846 to 0.00386 (Fig. 5, lowest curve). In experiments containing 2.45 ± 0.02 Torr of C_2H_2, addition of small amounts (up to 30 mTorr) of NO caused a slight increase in $\Phi\{CO\}$ (Fig. 5, middle curve). Futher additions of NO decreased $\Phi\{CO\}$; an addition of NO in excess of 18.6 Torr caused the quantum yield to approach the detection limit. A similar but more dramatic

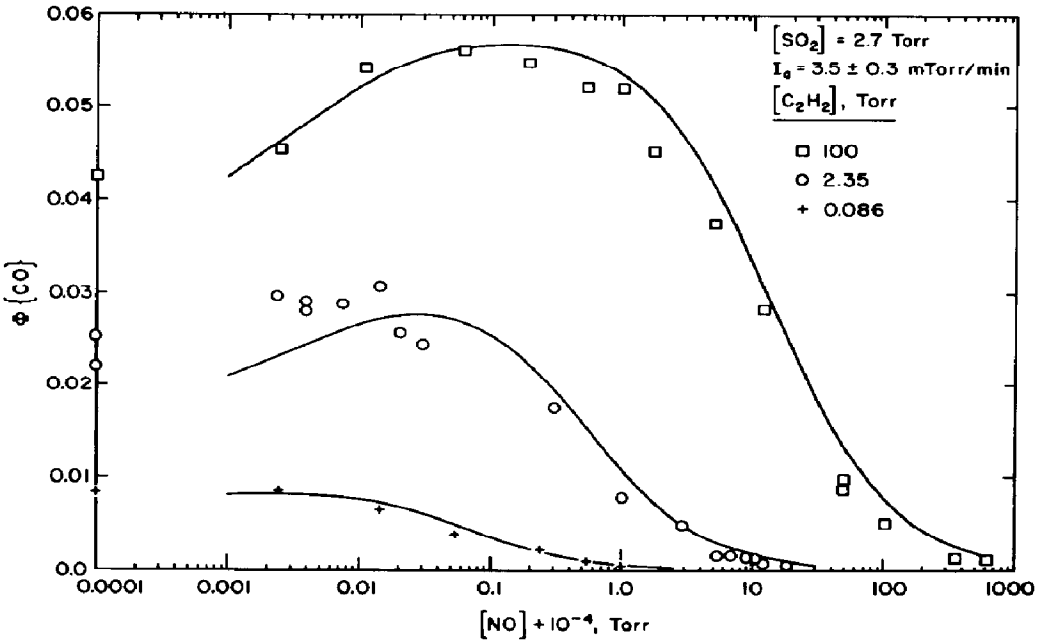

Fig. 5. Semilog plots of CO quantum yield *vs.* the NO pressure plus 10^{-4} Torr in the irradiation of SO_2–C_2H_2 mixtures in the presence of NO. The curves are theoretically computed from the rate coefficients listed in Table 1.

enhancement followed by decay was encountered when 100 Torr of C_2H_2 was present (Fig. 5, upper curve). Again once a sufficient amount of NO had been added the quantum yield decreased towards zero.

Another series of experiments was done with SO_2 at 2.7 ± 0.05 Torr. Water was added as a quenching gas at C_2H_2 pressures of 0.086, 2.35 and 100 Torr. The results of the experiments are shown in Fig. 6. The addition of H_2O vapor up to 18 Torr had little, if any, effect on $\Phi\{CO\}$ at the higher pressures of C_2H_2. However, with 0.086 Torr C_2H_2, the addition of H_2O vapor decreased $\Phi\{CO\}$ from 0.009 to a lower limiting value of 0.0017 at 18.3 Torr of H_2O.

The quenching studies described above using NO and H_2O were repeated in the presence of ~600 Torr of CO_2. With 2.8 ± 0.06 Torr of SO_2 and 2.8 ± 0.06 Torr of C_2H_2, [NO] was varied from 0.0322 to 34.8 Torr. The CO quantum yield again showed an increase at small pressures of added NO and the quenching curve obtained (Fig. 7) closely approximated the results obtained in the absence of CO_2. With 2.78 ± 0.02 Torr of SO_2, 0.086 ± 0.002 Torr of C_2H_2, and 620 ± 20 Torr of CO_2 present, $\Phi\{CO\}$ increased slightly from 0.00123 to 0.00157 as 13.2 Torr of H_2O was added. This increase is probably not significant as it lies within the available precision.

It was noticed that in runs in which only a few mTorr of NO were added some of the NO was consumed, presumably in secondary reactions. For runs with 2.34 ± 0.03 Torr of acetylene, 2.70 ± 0.05 Torr of SO_2, and

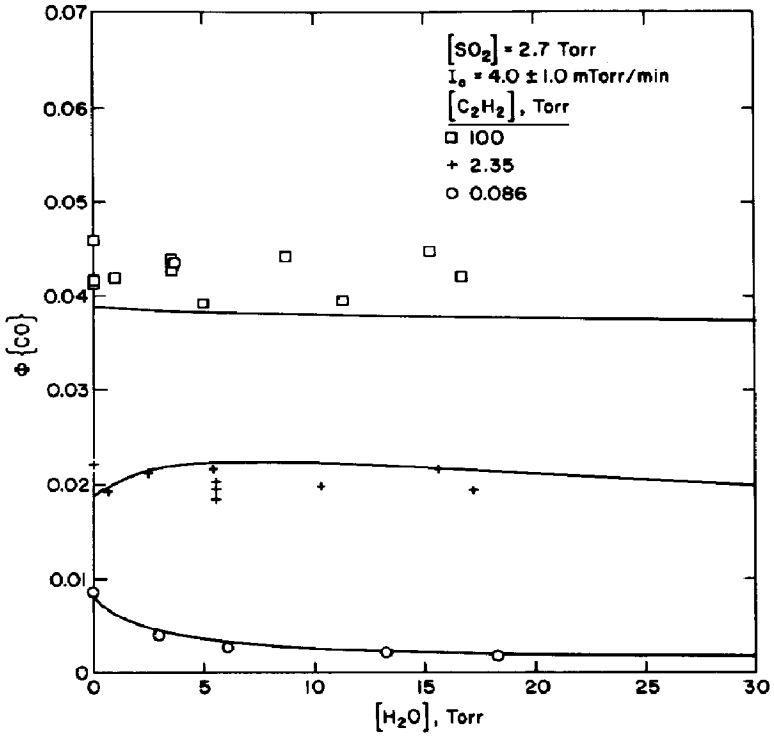

Fig. 6. Plots of CO quantum yield *vs.* H_2O pressure in the irradiation of SO_2–C_2H_2 mixtures in the presence of H_2O. The curves are theoretically computed from the rate coefficients listed in Table 1.

with 4.05 ± 0.03 mTorr of NO added, the loss of NO due to oxygen leakage into the cell was comparable to the loss by photolysis. It is believed that when the NO was transferred to the small known volume it reacted with any oxygen that had leaked in. Since the blank corrections were as large as the effect measured by photolysis only a rough estimate of the loss of NO can be given. For the above mentioned conditions, $\Phi\{CO\} \sim 0.025$ and the quantum yield of NO loss is about 0.0039.

Discussion

The major conclusions that can be drawn from this study are:

(1) SO_2 photoexcited at 3130 Å reacts with C_2H_2 to produce CO.

(2) The chemically reactive states are triplets, since CO production is readily eliminated in the presence of relatively small amounts of NO, a known efficient triplet quencher.

(3) At low total pressures, the exclusive triplet involved is the $^3B_1$ state which emits the phosphorescence, because $\Phi\{CO\}$ depends only on the ratio $[SO_2]/[C_2H_2]$ in accordance with previous information on this state. The other chemically reactive triplet state, SO_2^{**}, which is not quenched by SO_2, cannot be present at low pressures.

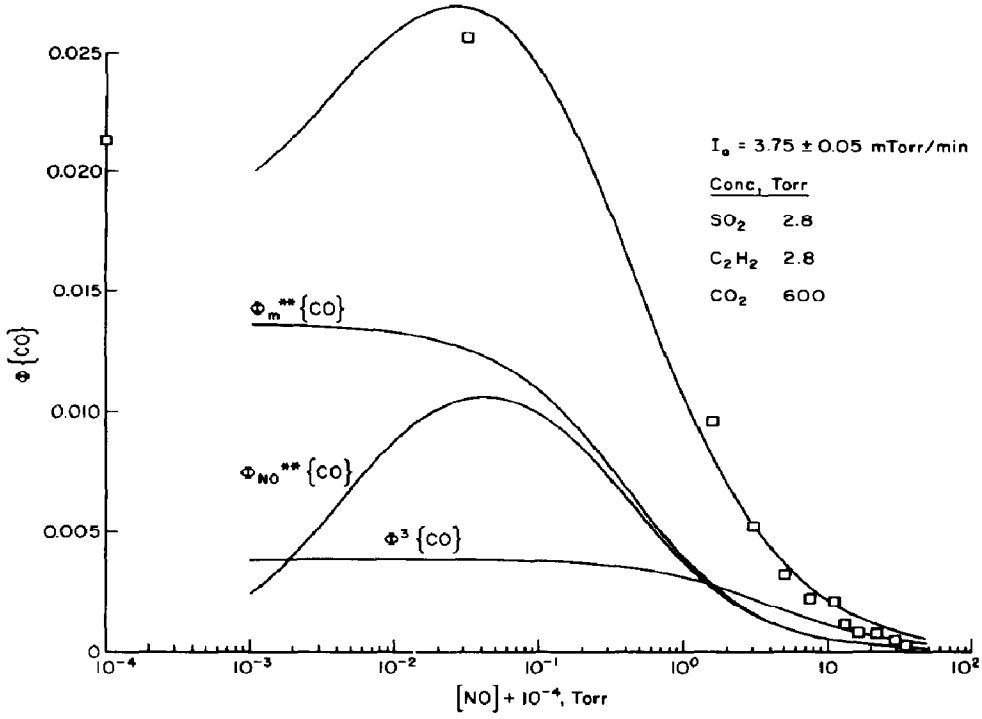

Fig. 7. Semilog plots of CO quantum yield *vs.* the NO pressure plus 10^{-4} Torr in the irradiation of SO_2–C_2H_2 mixtures in the presence of NO and 600 Torr CO_2. The curves are theoretically computed from the rate coefficients listed in Table 1. The contributions calculated from $\Phi^3\{CO\}$, $\Phi_M^{**}\{CO\}$, and $\Phi_{NO}^{**}\{CO\}$ are also shown.

(4) At high total pressures, with C_2H_2 as a minor constituent, $^3B_1$ is quenched and the CO is produced entirely from SO_2^{**}. This is demonstrated experimentally by the absence of any dependence of $\Phi\{CO\}$ on the SO_2 pressure.

(5) The presence of very small amounts of NO enhance $\Phi\{CO\}$ under some conditions. Thus there is a complex relationship existing in the triplet manifold of states.

The mechanism we have used to fit our results is one whose major steps are obtained from previous studies with a few added steps which the C_2H_2–SO_2 system needs. We shall abbreviate $SO_2(^3B_1)$ as $^3SO_2$, the fluorescing state as $^1SO_2$, and the longer-lived of the two states formed by absorption of radiation as SO_2^*. The chemically important non-emitting triplet state is SO_2^{**}, and $SO_2^\dagger$ represents the third triplet state introduced by Fatta *et al.* [31]. For convenience the entire mechanism is listed below.

$$SO_2 + h\nu \rightarrow SO_2^* \qquad \text{Rate} = I_a$$

$$SO_2^* \rightarrow {}^1SO_2 \tag{2a}$$

$$\rightarrow SO_2 \tag{2b}$$

$$SO_2^* + M \rightarrow SO_2^{**} + M \tag{3a}$$

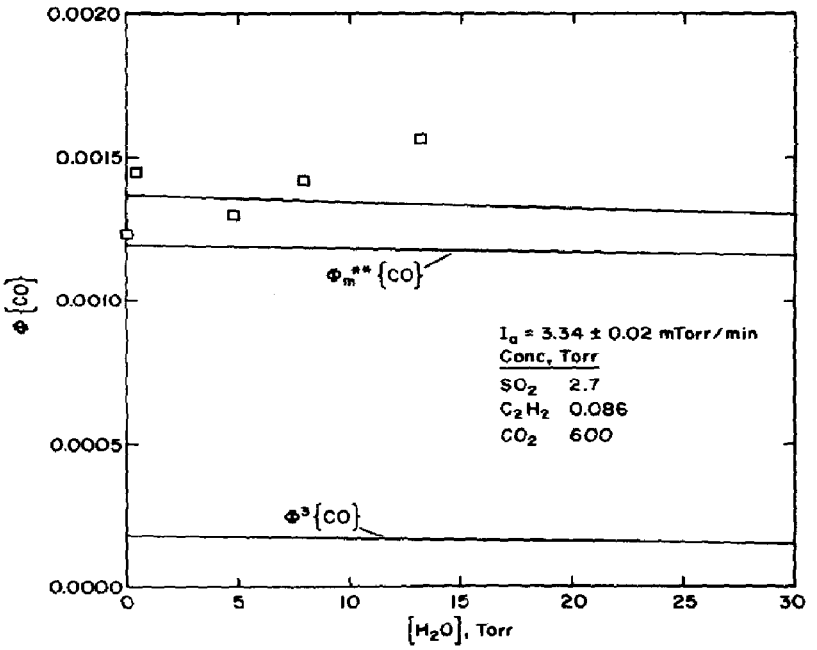

Fig. 8. Plots of CO quantum yield *vs.* H_2O pressure in the irradiation of SO_2–C_2H_2 mixtures in the presence of H_2O and 600 Torr CO_2. The curves are theoretically computed from the rate coefficients listed in Table 1. The contributions calculated from $\Phi^3\{CO\}$ and $\Phi_M^{**}\{CO\}$ are also shown.

	$\rightarrow SO_2 + M$		(3b)
$^1SO_2$	$\rightarrow SO_2 + h\nu_f$		(4)
$^1SO_2 + SO_2$	$\rightarrow$ removal		(5a)
$+ CO_2$	$\rightarrow$ removal		(5b)
$+ NO$	$\rightarrow$ removal		(5c)
$+ H_2O$	$\rightarrow$ removal		(5d)
$SO_2 + h\nu$	$\rightarrow {}^3SO_2$	Rate = αI_a	
$^3SO_2$	$\rightarrow SO_2 + h\nu_p$		(6)
$^3SO_2 + C_2H_2$	$\rightarrow CO$		(7a)
	$\rightarrow$ removal		(7b)
$^3SO_2 + SO_2$	$\rightarrow$ removal		(8a)
$+ CO_2$	$\rightarrow$ removal		(8b)
$+ NO$	$\rightarrow$ removal		(8c)
$+ H_2O$	$\rightarrow$ removal		(8d)
$SO_2^{**} + C_2H_2$	$\rightarrow CO$		(9)
$SO_2^{**} + NO$	$\rightarrow$ removal		(10)

$$SO_2^{**} \rightarrow \text{removal} \tag{11}$$

$$SO_2 + h\nu \rightarrow SO_2^{\dagger} \qquad \text{Rate} = \gamma I_a$$

$$SO_2^{\dagger} + NO \rightarrow SO_2^{**} + NO \tag{12}$$

$$SO_2^{\dagger} \rightarrow SO_2 \tag{13}$$

The longer lived state formed by absorption of radiation is presumably $^1B_1$. Because of its non-linear Stern–Volmer quenching plot, the state which fluoresces must be kinetically distinct and formed in a first-order process from SO_2^* [32]. Therefore we designate it $^1SO_2$. Whether this is a spectroscopically distinct entity or the result of a pertubation with the ground electronic state as proposed by Brus and McDonald [33] is immaterial from the viewpoint of photochemical kinetics where it behaves as if it were a distinct entity.

The SO_2^* state can be collisionally quenched to produce states other than $^1SO_2$ and possibly $^3SO_2$. Thus it can be quenched to the ground state or SO_2^{**} (and possibly $SO_2^{\dagger}$). In fact SO_2^{**} must come from this collisional quenching process as pointed out by Cehelnik *et al.* [28] and not from first-order processes, since it is absent at low pressures, but is very important at high pressures where it is not quenched by SO_2, CO_2, or H_2O. The SO_2^{**} state can be quenched by either C_2H_2 or NO. With C_2H_2, the quenching produces CO, at least part of the time. We do not have sufficient information to establish whether there is or is not a physical quenching process with C_2H_2 in which CO is not produced. Therefore for simplicity, we have omitted such a step.

The $^3SO_2$ is produced at a constant fraction, α, of the absorbed intensity, I_a. This is not to imply that $^3SO_2$ is produced directly on absorption but rather that the various modes of intersystem crossing which lead to $^3SO_2$ are such that the rate of production is independent of reaction pressure and α is a true constant [32]. Possibly $^3SO_2$ is produced from SO_2^*, but if so it must be produced in the same fraction of the time by first-order processes and collisional quenching of SO_2^* by C_2H_2, CO_2, and H_2O since the Stern–Volmer quenching curve for $^3SO_2$ is linear. It is extremely unlikely that every removal process of SO_2^* would lead to $^3SO_2$ being produced the same fraction of the time. More likely $^3SO_2$ comes from the $^1A_2$ state which is always collisionally quenched at our pressures. The $^3SO_2$ state is then collisionally quenched by any gas present in the system, reaction occurring part of the time if the quenching gas is C_2H_2. Under our conditions first-order removal steps are not important.

The evidence for the $SO_2^{\dagger}$ state is very circumstantial. Fatta *et al.* [31] needed a state which is very rapidly quenched by biacetyl but not quenched at all by most other gases (N_2, CO, CO_2, N_2O) to explain their data. This state is incorporated here to explain the increase in $\Phi\{CO\}$ when 30 mTorr of NO are added in both the absence and presence of excess CO_2. Thus a state is needed which is quenched by 30 mTorr of NO but is not quenched by CO_2. No other state has this property. Furthermore the

quenching process must lead to additional CO production. The simplest explanation is that the quenching of $SO_2^\dagger$ by NO produces SO_2^{**}. We have for simplicity assumed $SO_2^\dagger$ is produced at some constant fraction γ, of I_a, but there is no direct evidence that this is a true constant. The $SO_2^\dagger$ state is not chemically reactive and only serves to populate the reactive triplet, SO_2^{**}, when NO is present.

The mechanism predicts that

$$\Phi\{CO\} = \frac{\alpha k_{7a}[C_2H_2]}{k_7[C_2H_2] + k_8[X]} + \frac{k_9[C_2H_2]k_{3a}[M]}{(k_2 + k_3[M])(k_9[C_2H_2] + k_{10}[NO] + k_{11})} + \frac{\gamma k_9[C_2H_2]k_{13}[NO]}{(k_{13}[NO] + k_{14})(k_9[C_2H_2] + k_{10}[NO] + k_{11})} \quad \text{(I)}$$

In the first term [X] is $[SO_2]$, $[CO_2]$, [NO], or $[H_2O]$ as shown in reactions (8a - 8d). In the second term M is any gas that causes the intersystem crossing of SO_2^* to SO_2^{**}. The first term on the right hand side of the above expression is the contribution from the emitting triplet, $SO_2(^3B_1)$ which shall be called $\Phi^3\{CO\}$. The second term is the contribution from SO_2^{**} and shall be called $\Phi_M{}^{**}\{CO\}$. The third term is also from SO_2^{**} but this SO_2^{**} comes from $SO_2^\dagger$ and, in order to differentiate it, this fraction shall be designated $\Phi_{NO}{}^{**}\{CO\}$. It is important to remember however that we do not allow $SO_2^\dagger$ to react chemically so that there are two reactive states $^3SO_2$ and SO_2^{**} and one of these states, SO_2^{**}, comes from two precursor states. Thus:

$$\Phi\{CO\} = \Phi^3\{CO\} + \Phi_M{}^{**}\{CO\} + \Phi_{NO}{}^{**}\{CO\} \quad \text{(II)}$$

At low [M] with no NO the first term in eqn. (I) determines $\Phi\{CO\}$ and thus $\Phi\{CO\}^{-1}$ varies linearly with $[SO_2]/[C_2H_2]$ in the absence of other added gases. From a plot of $\Phi\{CO\}^{-1}$ *vs.* $[SO_2]/[C_2H_2]$ (Fig. 2) we can evaluate $k_7/k_{7a}\,\alpha$ to be 53 from the intercept, and by taking the ratio of intercept to slope, we find $k_7/k_{8a} = 23$. The value for α has been determined in numerous studies in Calvert's laboratory and elsewhere [15]. The best value at 3130 Å is 0.10 [17]. Thus $k_{7a}/k_7 = 0.189$.

In the presence of CO_2, but still at low total pressures, Fig. 9 shows that a plot of $\Phi\{CO\}^{-1}$ *vs.* $[CO_2]$ is linear. From the slope we obtain $k_{8b}/k_{7a}\,\alpha = 0.98$. Similarly, in the presence of H_2O at low total pressures, a plot of $\Phi\{CO\}^{-1}$ *vs.* $[H_2O]$ (Fig. 10) gives $k_{8d}/k_{7a}\,\alpha = 3.8$. From these rate coefficient ratios, the quenching efficiencies of the added gases relative to SO_2 can be obtained and they are listed in Table 1 along with the results of previous workers. Our value for $k_{8b}/k_{8a} = 0.42$ is higher than that obtained by Mettee [10] and Sidebottom *et al.* [40], but lower than that obtained by Stockburger *et al.* [32]. The value obtained here for k_{8d}/k_{8a} agrees well with previous work.

At higher added pressures, in the absence of NO, the CO yield from the emitting triplet, which is now determined, can be subtracted from the total quantum yield to obtain the rate constant ratios for the second term in eqn. (I):

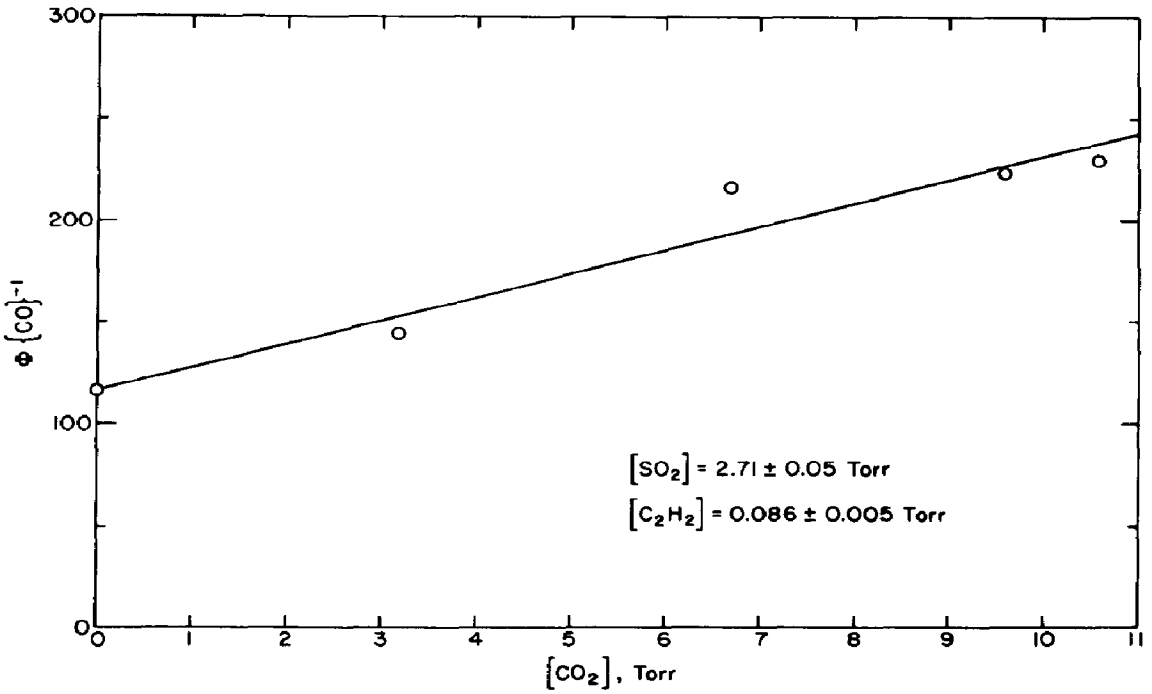

Fig. 9. Plot of reciprocal CO quantum yield *vs.* CO_2 pressure in the irradiation of SO_2–C_2H_2 mixtures in the presence of CO_2.

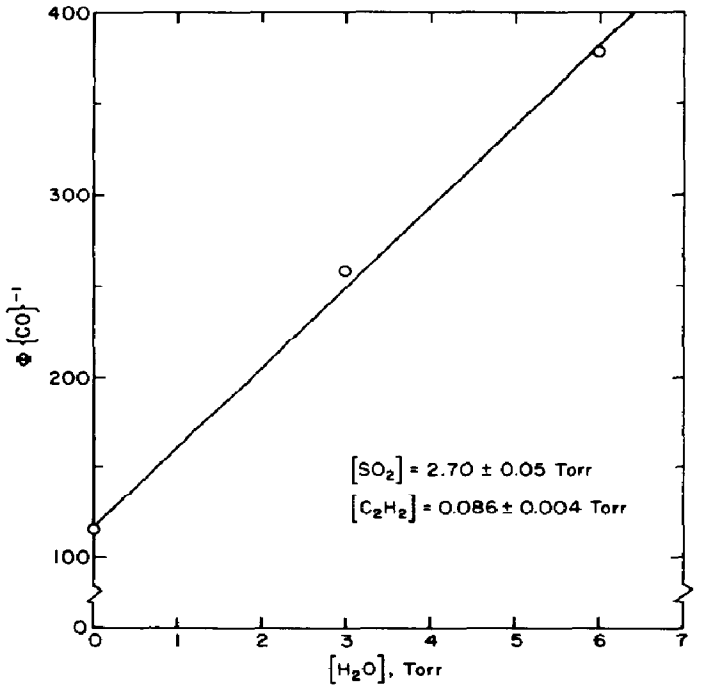

Fig. 10. Plot of reciprocal CO quantum yield *vs.* H_2O pressure in the irradiation of SO_2–C_2H_2 mixtures in the presence of H_2O.

TABLE 1

Summary of rate coefficient information

Ratio	Value	Units	M	Reference
α	0.10	None	—	Demerjian and Calvert [17]
k_{7a}/k_7	0.189	None	C_2H_2	This work
k_7/k_{8a}	23	None	C_2H_2	This work
k_{8b}/k_{8a}	0.42	None	CO_2	This work
	0.31	None	CO_2	Mettee [10]
	0.29	None	CO_2	Sidebottom *et al.* [40]
	0.55	None	CO_2	Stockburger *et al.* [32]
k_{8d}/k_{8a}	1.62	None	H_2O	This work
	2.28	None	H_2O	Sidebottom *et al.* [40]
	1.8	None	H_2O	Stockburger *et al.* [32]
k_{8c}/k_{8a}	80	None	NO	This work
	64	None	NO	Mettee [10]
	190	None	NO	Sidebottom *et al.* [40]
	~100	None	NO	Stockburger *et al.* [32]
k_2/k_3	73.1	Torr	C_2H_2	This work
	56.0	Torr	CO_2	This work
	~40	Torr	CO_2	Stockburger *et al.* [32]
	4.41	Torr	H_2O	This work
	~10	Torr	H_2O	Stockburger *et al.* [32]
k_3/k_{3a}	28.5	None	C_2H_2	This work
	45.2	None	CO_2	This work
	53.6	None	H_2O	This work
k_{11}/k_9	1.38	Torr	C_2H_2	This work
k_{11}/k_{10}	0.164	Torr	NO	This work
	0.34	Torr	NO	Cehelnik *et al.* [29]
γ	0.0193	None	—	This work
k_{13}/k_{12}	0.0045	Torr	NO	This work

$$\Phi_M^{**}\{CO\} = \Phi\{CO\} - \Phi^3\{CO\} = \frac{k_9[C_2H_2]k_{3a}[M]}{(k_2 + k_3[M])(k_9[C_2H_2] + k_{11})} \quad \text{(III)}$$

A plot of $(\Phi\{CO\} - \Phi^3\{CO\})^{-1}$ *vs.* $[C_2H_2]^{-1}$ is shown in Fig. 11 for runs done in the presence of excess CO_2 so that $[M] \simeq [CO_2]$. The slopes of the lines give $(k_2 + k_3[M])k_{11}/k_{3a}k_9[M]$, while the intercepts give $(k_2 + k_3[M])/k_{3a}[M]$. The ratio of slope to intercept gives k_{11}/k_9. The majority of runs were done at 600 Torr of CO_2 but the limited series at 300 and 100 Torr of CO_2 are also plotted. The intercepts of these plots with different pressures of CO_2 may be used to obtain an estimate of k_2/k_3 and k_3/k_{3a}. If the intercept for the 100 Torr plot is divided by that for the 600 Torr plot we can obtain k_2/k_3 and by putting this back in one of the individual expressions for the intercept we obtain k_3/k_{3a}. The same procedure can be used with the 300 and 600 or 300 and 100 Torr runs. This procedure is subject to a large error since the quantum yields are very low in the presence of large amounts of CO_2 when the C_2H_2

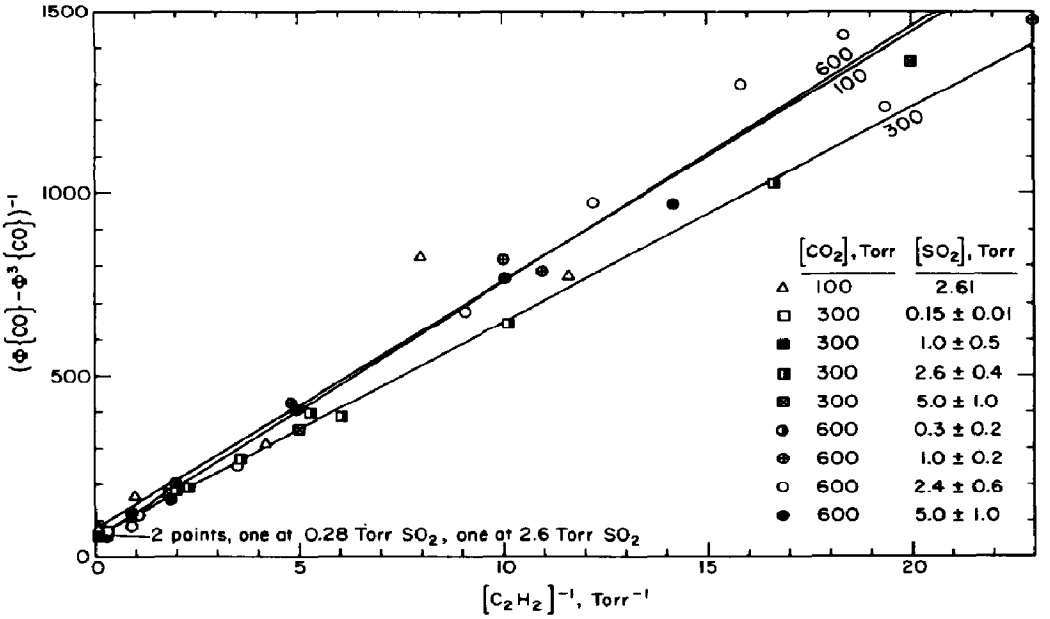

Fig. 11. Plot of $(\Phi\{CO\}-\Phi^3\{CO\})^{-1}$ *vs.* the reciprocal C_2H_2 pressure in the irradiation of SO_2–C_2H_2 mixtures in the presence of excess CO_2.

pressure was low. However, the results using various combinations of the 100, 300, and 600 Torr intercepts agreed with each other and when varied by small amounts no improvement in fit to the actual quenching curves was obtained. The rate constant ratios obtained are listed in Table 1. The value of $k_2/k_3 = 56$ is in satisfactory agreement with the value of ~40 which can be deduced from the data of Stockburger *et al.* [32].

With high pressures of acetylene in the absence of added gases, the rate constants k_2/k_3 and k_3/k_{3a} can be evaluated for C_2H_2 as the main quenching gas, *i.e.* $[C_2H_2] \simeq [M]$. The points on a plot of $(\Phi\{CO\} - \Phi^3\{CO\})^{-1}$ *vs.* $1/[C_2H_2]$ above 10 Torr can be used to evaluate the ratios. Since under these conditions $k_{11} \ll k_9[C_2H_2]$:

$$(\Phi\{CO\} - \Phi^3\{CO\})^{-1} \simeq k_3/k_{3a} + k_2/k_{3a}[C_2H_2] \qquad (IV)$$

Figure 12 shows the plot obtained and Table 1 lists the rate constant ratios.

H_2O quenches $SO_2(^3B_1)$ rather efficiently, yet there was no decrease in $\Phi\{CO\}$ upon the addition of up to 18 Torr of H_2O to a mixture of 2.7 Torr SO_2 and 2.34 Torr C_2H_2. A decrease would be expected based on the rate coefficients obtained so far. There must be a compensating mechanism which tends to enhance $\Phi\{CO\}$ when H_2O is added, and thus offset the decrease expected from quenching of the $^3B_1$ state. The most obvious step is that H_2O efficiently quenches SO_2^* to produce SO_2^{**}. Thus in the

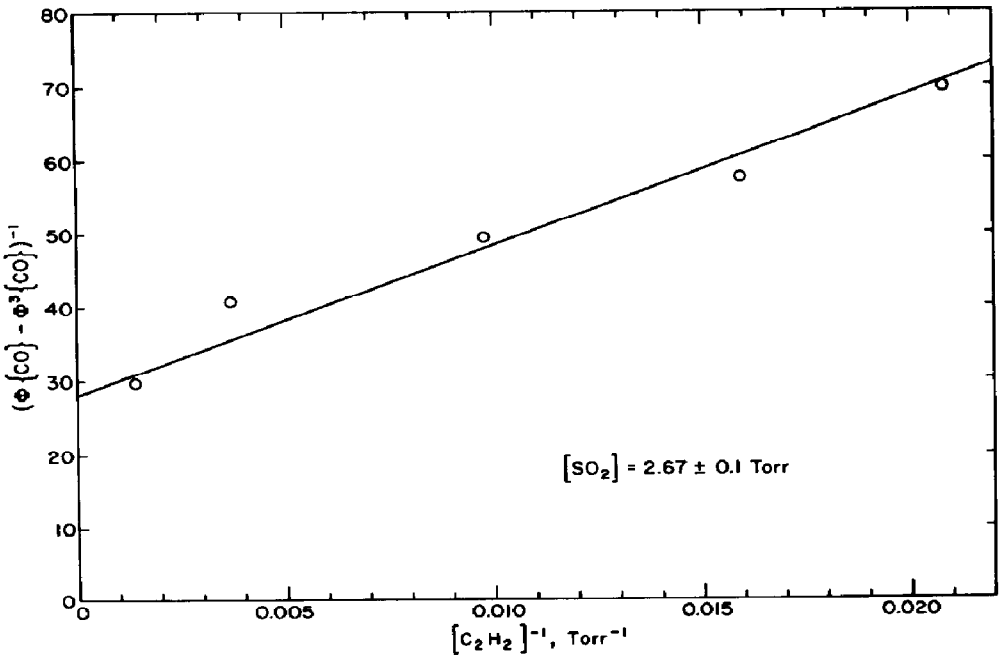

Fig. 12. Plot of $(\Phi\{CO\} - \Phi^3\{CO\})^{-1}$ *vs.* the reciprocal C_2H_2 pressure in the irradiation of SO_2–C_2H_2 mixtures at high C_2H_2 pressures.

same manner as for CO_2 or C_2H_2, the rate constant ratios k_3/k_{3a} and k_2/k_{3a} can be obtained for H_2O. A plot of $(\Phi\{CO\} - \Phi^3\{CO\})^{-1}$ *vs.* $1/[H_2O]$ (Fig. 13), along with previously obtained rate coefficient ratios give these rate constant ratios, and they are listed in Table 1.

The value of $k_2/k_3 = 4.41$ obtained here for H_2O is too small to be consistent with that found by Stockburger *et al.* [32] by direct observation. Thus there appears to be an additional step needed to enhance $\Phi\{CO\}$ when H_2O is added. From our results, it is not certain what this step is, but a good possibility would be quenching of $SO_2^\dagger$ by H_2O to produce SO_2^{**}. Such a hypothesis is consistent with the interpretation of Fatta *et al.* [31], who required that either $SO_2^\dagger$ or SO_2^{**} be efficiently quenched by H_2O vapor. They assumed that SO_2^{**} was the state quenched, but our results show that this is not so. Presumably it is the $SO_2^\dagger$ state which is efficiently quenched by H_2O vapor. However, this interpretation is so tentative at the present time, that we will ignore it, and just use $k_2/k_3 = 4.4$ for H_2O vapor.

SO_2 was found to be very inefficient at promoting the crossing of SO_2^* to SO_2^{**} over the range of pressures used (maximum pressure of 19.3 Torr). The treatment which was used for water could not be used for SO_2, and SO_2 acted only as a quencher of $SO_2(^3B_1)$ in the pressure range investigated.

When NO is added to the system the $SO_2^\dagger$ state becomes important. However, for runs at 0.086 ± 0.004 Torr of C_2H_2 and SO_2 pressures of 2.70 ± 0.06 Torr the emitting triplet accounts for over 95% of the CO.

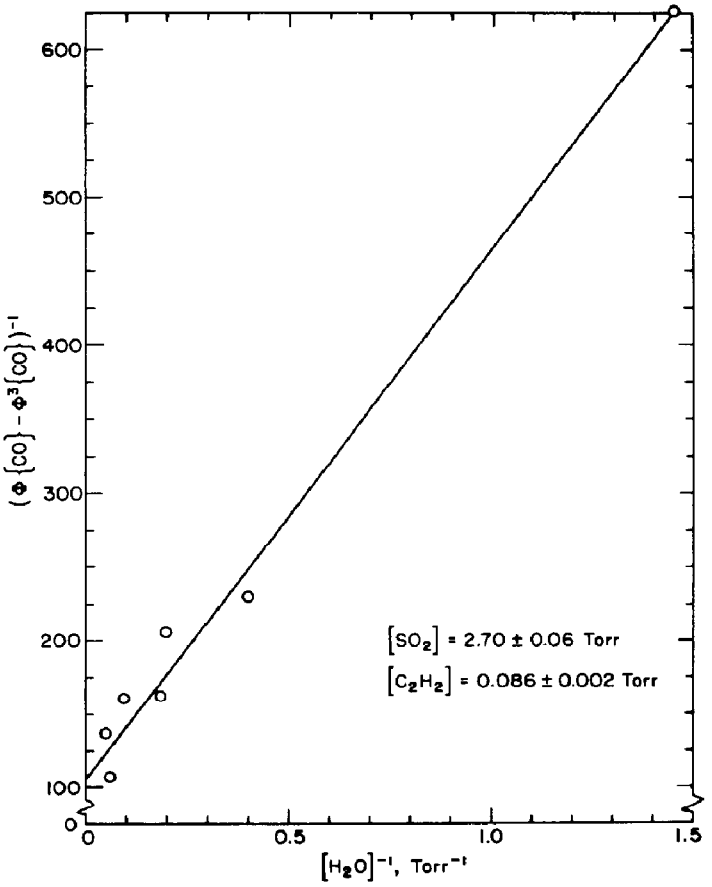

Fig. 13. Plot of $(\Phi\{CO\} - \Phi^3\{CO\})^{-1}$ *vs.* the reciprocal H_2O pressure in the irradiation of SO_2–C_2H_2 mixtures in the presence of H_2O.

Therefore, the first term in eqn. (I) is the only important one, and a plot of $\Phi\{CO\}^{-1}$ *vs.* $1/[NO]$, shown in Fig. 14, allows evaluation of k_{8c}/k_{8a}. The value obtained, 80, listed in Table 1 agrees reasonably well with that of Mettee [10], is consistent with that of Stockburger *et al.* [32] but is much lower than the value of 190 obtained upon direct excitation of the triplet [40].

The presence of the $SO_2^{\dagger}$ state is most noticeable when the pressure of C_2H_2 is high and very small amounts of NO are added. Under these conditions $k_{11} + k_{10}[NO] \ll k_9[C_2H_2]$, and the expression for $\Phi_{NO}^{**}\{CO\}^{-1}$ becomes:

$$\Phi_{NO}^{**}\{CO\}^{-1} = (\Phi\{CO\} - \Phi^3\{CO\} - \Phi_M^{**}\{CO\})^{-1}$$
$$= \gamma^{-1} + k_{13}/\gamma k_{12}[NO] \qquad (V)$$

A plot of $\Phi_{NO}^{**}\{CO\}^{-1}$ for very low pressures of NO and 100 Torr C_2H_2 is shown in Fig. 15. The limited data are fitted by a straight line and from the slope and intercept γ and k_{13}/k_{12} can be evaluated. Their values are listed in Table 1.

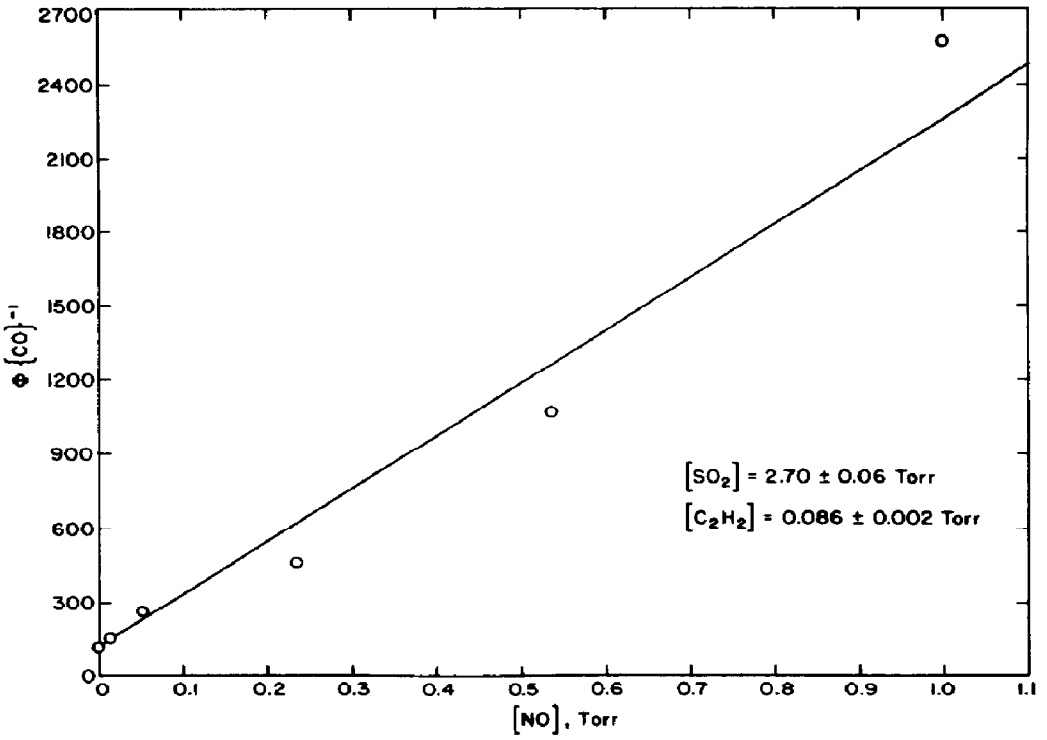

Fig. 14. Plot of reciprocal CO quantum yield *vs.* NO pressure in the irradiation of SO_2–C_2H_2 mixtures in the presence of NO with $[C_2H_2]$ = 0.086 ± 0.002 Torr.

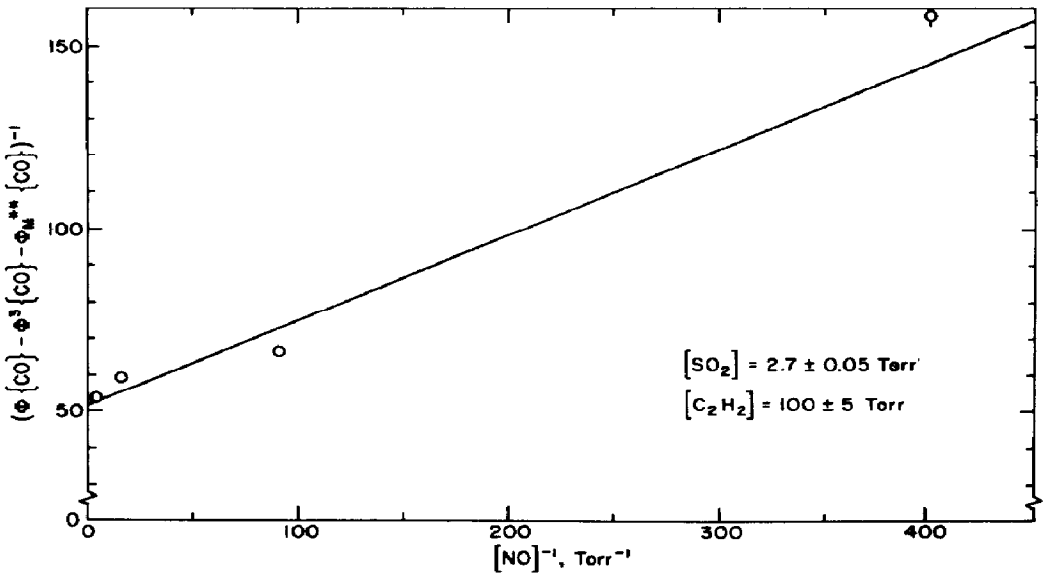

Fig. 15. Plot of $(\Phi\{CO\} - \Phi^3\{CO\} - \Phi_{M^{**}}\{CO\})^{-1}$ *vs.* the reciprocal NO pressure in the irradiation of SO_2–C_2H_2 mixtures in the presence of NO with $[C_2H_2]$ = 100 ± 5 Torr.

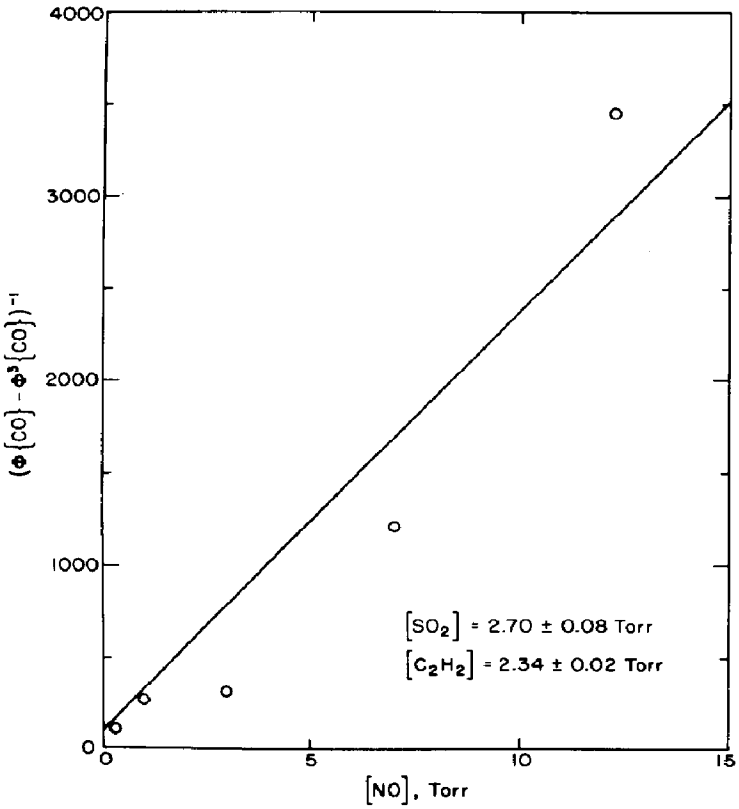

Fig. 16. Plot of $(\Phi\{CO\} - \Phi^3\{CO\})^{-1}$ *vs.* NO pressure in the irradiation of SO_2–C_2H_2 mixtures in the presence of NO with $[C_2H_2]$ = 2.34 ± 0.02 Torr.

An evaluation of the quenching efficiency of NO on SO_2^{**} can be made when the NO pressure is relatively high so that $SO_2^{\dagger}$ is completely quenched, and $[C_2H_2]$ is sufficiently low to permit competition of C_2H_2 and NO for SO_2^{**}, but $[C_2H_2]$ is still sufficiently high so that CO production is not predominantly from $SO_2(^3B_1)$. The optimum C_2H_2 pressure is about 2 Torr. Under these conditions, $k_3[M]$ is also negligible compared to k_2, and the rate law becomes

$$(\Phi\{CO\} - \Phi^3\{CO\})^{-1} = \left(1 + \frac{k_{10}[NO]}{k_9[C_2H_2]} + \frac{k_{11}}{k_9[C_2H_2]}\right)\left(\gamma + \frac{k_{3a}[M]}{k_2}\right) \quad \text{(VI)}$$

Figure 16 shows a plot of $(\Phi\{CO\} - \Phi^3\{CO\})^{-1}$ *vs.* [NO] for $[C_2H_2]$ = 2.34 Torr. If $\gamma + k_{3a}[M]/k_2$ is not much influenced by changes in the NO pressure, then the plot should be linear. The limited data are badly scattered, but we force a straight line through them and equate the ratio of slope to intercept of 2.26 $Torr^{-1}$ to $(k_{10}/k_9[C_2H_2])/(1 + k_{11}/k_9[C_2H_2])$. From the already evaluated rate constants k_{11}/k_{10} can be estimated to be ~0.16 Torr. This value has considerable uncertainty, but still is more than a factor of two smaller than that evaluated by Cehelnik *et al.* [29].

However, in the presence of NO, the mechanism of Cehelnik *et al.* [29] never fitted the data well; there was always more chemical product than could be accounted for by their mechanism. They concluded that there must be an additional source of chemical product. From the results here, we know this source to be the $SO_2^{\ddagger}$ state which they did not include. Had they included it, their value for k_{11}/k_{10} would have been reduced considerably, probably by a factor of 2 or more. With this realization, it can be concluded that the results from their and our study regarding the quenching of SO_2^{**} by NO are in good agreement.

The rate constant ratios obtained in this study (Table 1) were substituted into expression (I), and theoretical values of Φ {CO} computed. The theoretically computed curves are drawn in Figs. 1, 3, and 5 - 8. In some cases the contributions from the individual states are also shown. The fit is satisfactory except that the calculated values tend to be slightly low in some cases. However, the general trend is predicted and the shape is reproduced in all cases. For some of the curves, most notably Fig. 1 (curve b) an attempt was made to curve fit by changing k_2/k_{3a}. This yielded no improvement even with a large variation. Therefore some of the rate constant ratios such as those involving reactions (2) and (3), are subject to large uncertainty.

Conclusion

It is clear that the SO_2–C_2H_2 system is very complex and involves the participation of several electronic states. As such the proposed mechanism must be considered as a simplification necessitated to maintain some degree of tractability. However, the mechanism does represent a good approximation to reality and with it we are able to reproduce the experimental observations very satisfactorally. In most cases rate constant ratios obtained agree well with those of other workers. The inadequacy of the mechanism to exactly reproduce the data in all cases probably reflects the participation of reactions which have not been included. Most importantly, this study demonstrates once again that for many systems involving photoexcited SO_2 one cannot rely exclusively on the emitting states to explain the data.

The SO_2^{**} state which is needed to explain CO production at high pressures should be considered firmly established as important in the photochemistry of SO_2. On the other hand, the existence of the $SO_2^{\ddagger}$ state is more tentative. However, it appears to be necessary to explain the phosphorescence of biacetyl photosensitized by SO_2 [31] as well as the excess chemical yields in the SO_2–CO system [29] and in this study.

Acknowledgements

We wish to thank Mr. Kenneth Partymiller for helpful discussions. This work was supported by the Center for Air Environment Studies at Penn State University for which we are grateful.

References

1 H. D. Mettee, J. Chem. Phys., 49 (1968) 1784.
2 S. J. Strickler and D. B. Howell, J. Chem. Phys., 49 (1968) 1947.
3 T. N. Rao, S. S. Collier and J. G. Calvert, J. Am. Chem. Soc., 91 (1969) 1609.
4 T. N. Rao, S. S. Collier and J. G. Calvert, J. Am. Chem. Soc., 91 (1969) 1616.
5 K. F. Greenough and A. B. F. Duncan, J. Am. Chem. Soc., 83 (1961) 555.
6 R. B. Caton and A. B. F. Duncan, J. Am. Chem. Soc., 90 (1968) 1945.
7 H. D. Mettee, J. Am. Chem. Soc., 90 (1968) 2972.
8 S. Okuda, T. N. Rao, D. H. Slater and J. G. Calvert, J. Phys. Chem., 73 (1969) 4412.
9 S. S. Collier, A. Morikawa, D. H. Slater, J. G. Calvert, G. Reinhardt and E. Damon, J. Am. Chem. Soc., 92 (1970) 217.
10 H. D. Mettee, J. Phys. Chem., 73 (1969) 1071.
11 F. S. Dainton and K. T. Ivin, Trans. Faraday Soc., 46 (1950) 374.
12 F. S. Dainton and K. T. Ivin, Trans. Faraday Soc., 46 (1950) 382.
13 R. B. Timmons, Photochem. Photobiol., 12 (1970) 219.
14 F. B. Wampler, A. Horowitz and J. G. Calvert, J. Am. Chem. Soc., 94 (1972) 5523.
15 R. A. Cox, J. Photochem., 2 (1973/74) 1.
16 R. D. Penzhorn and G. H. Gusten, Z. Naturforsch., 27a (1972) 1401.
17 K. L. Demerjian and J. G. Calvert, Int. J. Chem. Kinet., 7 (1975) 45.
18 G. E. Jackson and J. G. Calvert, J. Am. Chem. Soc., 93 (1971) 2593.
19 C. C. Badcock, H. W. Sidebottom, J. G. Calvert, G. W. Reinhardt and E. K. Damon, J. Am. Chem. Soc., 93 (1971) 3115.
20 K. L. Demerjian, J. G. Calvert and D. L. Thorsell, Int. J. Chem. Kinet., 6 (1974) 829.
21 H. W. Sidebottom, C. C. Badcock, J. G. Calvert, B. R. Rabe and E. K. Damon, J. Am. Chem. Soc., 93 (1971) 3121.
22 K. Otsuka and J. G. Calvert, J. Am. Chem. Soc., 93 (1970) 2581.
23 H. W. Sidebottom, C. C. Badcock, J. G. Calvert, G. W. Reinhardt, B. R. Rabe and E. K. Damon, J. Am. Chem. Soc., 93 (1971) 2587.
24 A. Horowitz and J. G. Calvert, Int. J. Chem. Kinet., 4 (1972) 175.
25 A. Horowitz and J. G. Calvert, Int. J. Chem. Kinet., 4 (1972) 191.
26 F. B. Wampler, J. G. Calvert and E. K. Damon, Int. J. Chem. Kinet., 5 (1973) 107.
27 F. B. Wampler, K. Otsuka, J. G. Calvert and E. K. Damon, Int. J. Chem. Kinet., 5 (1973) 669.
28 E. Cehelnik, C. W. Spicer and J. Heicklen, J. Am. Chem. Soc., 93 (1971) 5371.
29 E. Cehelnik, J. Heicklen, S. Braslavsky, L. Stockburger, III and E. Mathias, J. Photochem., 2 (1973) 31.
30 S. Braslavsky and J. Heicklen, J. Am. Chem. Soc., 94 (1972) 4864.
31 A. M. Fatta, E. Mathias, J. Heicklen, L. Stockburger, III and S. Braslavsky, J. Photochem., 2 (1973) 119.
32 L. Stockburger, III, S. Braslavsky and J. Heicklen, J. Photochem., 2 (1973) 15.
33 L. E. Brus and J. R. McDonald, Chem. Phys. Lett., 21 (1973) 283; J. Chem. Phys., 61 (1974) 97.
34 A. D. Walsh, J. Chem. Soc., (1953) 2266.
35 F. C. James, J. A. Kerr and J. P. Simons, Chem. Phys. Lett., 25 (1974) 431.
36 K. Chung, J. G. Calvert and J. W. Bottenheim, Int. J. Chem. Kinet., 7 (1975) 161.
37 M. Luria, R. G. de Pena, K. J. Olszyna and J. Heicklen, J. Phys. Chem., 78 (1974) 325.
38 M. Luria and J. Heicklen, Can. J. Chem., 52 (1974) 3451.
39 R. Renaud and L. C. Leitch, Can. J. Chem., 32 (1954) 549.
40 H. W. Sidebottom, C. C. Badcock, G. E. Jackson, J. G. Calvert, G. W. Reinhardt and E. K. Damon, Environ. Sci. Technol., 6 (1972) 72.